Published in final edited form as:
J Biol Chem. 2002 November 22; 277(47): 44660–44669. doi:10.1074/jbc.M203584200.

Transient State Kinetic Investigation of 5-Aminolevulinate Synthase Reaction Mechanism*

Junshun Zhang[‡] and **Gloria C. Ferreira**[‡,§,¶,‖]

[‡]Department of Biochemistry and Molecular Biology, College of Medicine, University of South Florida, Tampa, Florida 33612

[§]Institute for Biomolecular Science, University of South Florida, Tampa, Florida 33612

[¶]H. Lee Moffitt Cancer Center and Research Institute, University of South Florida, Tampa, Florida 33612

Abstract

5-Aminolevulinate synthase (ALAS), a pyridoxal 5′-phosphate-dependent enzyme, catalyzes the first, and regulatory, step of the heme biosynthetic pathway in nonplant eukaryotes and some bacteria. 5-Aminolevulinate synthase is a dimeric protein having an ordered kinetic mechanism with glycine binding before succinyl-CoA and with aminolevulinate release after CoA and carbon dioxide. Rapid scanning stopped-flow absorption spectrophotometry in conjunction with multiple turnover chemical quenched-flow kinetic analyses and a newly developed CoA detection method were used to examine the ALAS catalytic reaction and identify the rate-determining step. The reaction of glycine with ALAS follows a three-step kinetic process, ascribed to the formation of the Michaelis complex and the pyridoxal 5′-phosphate-glycine aldimine, followed by the abstraction of the glycine *pro*-R proton from the external aldimine. Significantly, the rate associated with this third step (k_3 = 0.002 s^{-1}) is consistent with the rate determined for the ALAS-catalyzed removal of tritium from [2-$^3H_2$]glycine. Succinyl-CoA and acetoacetyl-CoA increased the rate of glycine proton removal ~250,000-and 10-fold, respectively, supporting our previous proposal that the physiological substrate, succinyl-CoA, promotes a protein conformational change, which accelerates the conversion of the external aldimine into the initial quinonoid intermediate (Hunter, G. A., and Ferreira, G. C. (1999) *J. Biol. Chem*. 274, 12222–12228). Rapid scanning stopped-flow and quenched-flow kinetic analyses of the ALAS reaction under single turnover conditions lend evidence for two quinonoid reaction intermediates and a model of the ALAS kinetic mechanism in which product release is at least the partially rate-limiting step. Finally, the carbonyl and carboxylate groups of 5-aminolevulinate play a major protein-interacting role by inducing a conformational change in ALAS and, thus, possibly modulating product release.

5-Aminolevulinate synthase (ALAS)[1] (EC 2.3.1.37) catalyzes the first step in heme biosynthesis in nonplant eukaryotes and some bacteria. This reaction involves the

*This work was supported by the National Institutes of Health and by the Chiles Endowment Biomedical Research Program of the Florida Department of Health. The rapid scanning stopped flow equipment was purchased with National Science Foundation Multi-User Biological Equipment Grant DBI-9604675.

‖To whom correspondence should be addressed: Dept. of Biochemistry and Molecular Biology, College of Medicine, University of South Florida, 12901 Bruce B. Downs Blvd., Tampa, FL 33612. Tel.: 813-974-5797; Fax: 813-974-0504; gferreir@hsc.usf.edu.

[1]The abbreviations used are: ALAS, 5-aminolevulinate synthase; ALA, 5-aminolevulinate; PLP, pyridoxal 5′-phosphate; AONS, 8-amino-7-oxononanoate synthase; MOPS, 4-morpholinepropanesulfonic acid; Tricine, *N*-[2-hydroxy-1,1-bis(hydroxymethyl)ethyl]glycine.

condensation of glycine and succinyl-CoA to produce 5-aminolevulinate (ALA), CoA, and carbon dioxide (1–3). Mammals encode two distinct ALAS isoforms (1), a non-tissue-specific ALAS (ALAS1) and an erythroid-specific ALAS (ALAS2) (4–6). Defects in the human ALAS2 gene have been implicated in the erythropoietic disorder, X-linked sideroblastic anemia (7).

ALAS requires pyridoxal 5′-phosphate (PLP) as an essential cofactor (1). PLP-dependent enzymes have been classified according to different criteria (*e.g.* homology in sequence alignments in parallel with similar reaction specificity (C-α, C-β, or C-γ as the reactive C in the amino acid substrate) and, more recently, fold types derived from three-dimensional structures (8–10)). ALAS belongs to the α-oxoamine synthase subfamily of PLP-dependent enzymes that catalyze the condensation of an amino acid and a carboxylic acid CoA thioester with the concomitant decarboxylation of the amino acid (1, 11–14).

The members of the α-oxoamine synthase subfamily, which include ALAS, 8-amino-7-oxononanoate synthase (AONS) (11), 2-amino-3-ketobutyrate CoA ligase (12), and serine palmitoyltransferase (13), are grouped within the α-family (8) or within class II of fold type I of the PLP-dependent enzyme superfamily (9, 10). Alignment of the amino acid sequences of the α-oxoamine synthase enzymes reveals several functionally important, highly conserved residues, although these enzymes share low overall sequence identity (11). In addition, α-oxoamine synthase enzymes appear to possess similar catalytic mechanisms; thus, understanding the ALAS mechanistic pathway directly impacts on the mechanistic interpretation of all enzymes of the α-oxoamine synthase family.

The results of the original radiolabeling studies with *Rhodobacter spheroides* ALAS provided the critical information to develop a model of the ALAS catalytic reaction mechanism (Scheme 1) (15–17). First, as with other PLP-dependent enzymes, a transaldimination reaction occurs between the substrate (glycine in the case of ALAS) and the internal aldimine, formed between the aldehyde group of PLP and an active site lysine residue. Following the transaldimination reaction and formation of the external aldimine, the *pro*-R proton of glycine is removed, yielding a transient quinonoid species in the presence of succinyl-CoA (17–20). This quinonoid intermediate reacts with succinyl-CoA to form, upon removal of the CoA group, an aldimine to α-amino-β-ketoadipate. Subsequently, cleavage of the C-α–carboxylate bond leads to a stabilized quinonoid intermediate (20). A proton is then returned to the C-5 position of the aldimine between PLP and ALA. Finally, the aldimine dissociates to yield ALA and the holoenzyme.

ALAS functions as a homodimer; residues from both sub-units contribute to the active site (21). Specifically, Lys^{313} of murine ALAS2 forms a Schiff base linkage with the PLP cofactor in the absence of the glycine substrate (22). Further, Lys^{313} is postulated to function as the catalytic base in the proton abstraction from the external aldimine intermediate to form the quinonoid intermediate (19). Asp^{279} has been identified as a crucial residue in ALAS catalysis by enhancing the electron withdrawing capacity of the PLP cofactor through the stabilization of the protonated form of the PLP pyridinium ring nitrogen (23). In addition, Arg^{439} appears to play a role in recognition and binding of glycine through an ionic bond between its guanidinium side chain and the carboxylate of the glycine substrate (24).

Although the α-oxoamine synthase enzymes are of central importance in the metabolism of heme, biotin, ceramides, and sphingolipids, their enzymatic mechanisms have not been completely resolved. The characteristic absorption spectral bands of the PLP cofactor and the covalent substrate-coenzyme intermediates make possible their spectroscopic monitoring. In addition, examining the formation of the three products (CoA, carbon

dioxide, and ALA) can be instrumental in unraveling the reaction mechanism. With these observations in mind, we performed a series of pre-steady-state kinetic studies, involving stopped-flow spectroscopy and chemical quenched flow, in order to provide an in depth transient kinetic analysis aimed at defining the elementary steps of the ALAS reaction pathway and dissecting its rate-limiting step. Multiwavelength kinetics and global analysis of pre-steady-state (single turnover and multiturnover) kinetic data revealed 1) the presence of two quinonoid intermediates, 2) an over 250,000-fold increase in the glycine proton removal and formation of the first quinonoid intermediate in the presence of succinyl-CoA, and 3) that the rate-determining step of the overall reaction is dictated by the release of the ALA product.

EXPERIMENTAL PROCEDURES

Reagents

The following reagents were from Sigma: DEAE-Sephacel, β-mercaptoethanol, PLP, bovine serum albumin, acetoacetyl-CoA, succinyl-CoA, acetylacetone, ALA-hydrochloride, 5-aminopentanoate, HEPES-free acid, MOPS, Tricine, thiamin pyrophosphate, sodium oxalacetate, sodium pyruvate, porcine heart pyruvate dehydrogenase, *Thermoplasma acidophilum* citrate synthase, and the bicinchoninic acid protein determination kit. Ultrogel AcA-44 was obtained from IBF Biotechnics. Glycerol, glycine, disodium ethylenediamine tetraacetic acid dihydrate, ammonium sulfate, magnesium chloride hexahydrate, and potassium hydroxide were purchased from Fisher. SDS-PAGE reagents were supplied by Bio-Rad.

Overexpression, Purification, and Analysis of ALAS

Recombinant murine ALAS2 was overproduced and purified from *Escherichia coli* DH5α cells harboring pGF23, an ALAS overexpression plasmid, as previously described (25), with the following modifications of the purification procedure. The DEAE-Sephacel column (2.7 × 11 cm) was loaded with the protein sample collected from the Ultrogel AcA-44 column (2.8 × 38 cm) and washed with buffer A (20 mM potassium phosphate, pH 7.5, 5 mM β-mercaptoethanol, 1 mM EDTA, 20 μM PLP, 10% glycerol) until the collected protein fractions had values for absorbance at 280 nm lower than 0.1. The elution of ALAS from the DEAE-Sephacel column was with 120 ml of buffer A containing 75 mM potassium chloride.[2] The purified ALAS was concentrated by pressurized dialysis in an Amicon 8050 stir cell equipped with a YM30 membrane. The concentrated, purified ALAS protein, typically at concentration of 550–800 μM, was stored under liquid nitrogen in Nalgene 2.0-ml polypropylene cryovials until use. Protein purity was assessed by SDS-PAGE (26) and was never less than 95%. Protein concentration was determined by the bicinchoninic acid method using serum albumin as a standard as described previously (23), and all protein concentrations are reported based on a subunit molecular mass of 56,000 Da. Enzymatic activity was determined using a continuous spectrophotometric assay as previously described (27).

Rapid Scanning Stopped-flow Spectroscopy

Rapid scanning stopped-flow kinetic measurements were performed using a model RSM-1000 stopped-flow spectrophotometer (OLIS Inc.). This instrument has a 2-ms dead time, a 4.0-mm path length, and a thermostatted observation chamber. In general, scan spectra covering the wavelength range of 325–545 nm were collected at a rate of 1000 scans/s. For reactions longer than 5 s, the scan speed was adjusted to 62 scans/s to reduce

[2]A. Cheltsov and G. C. Ferreira, unpublished data.

data files to a manageable level. A fixed 0.6-mm slit was used to collect data. A circulating water bath controlled thermostatically at 20 or 30 °C was used to maintain the temperature of the loading syringes (containing the reactants) and the stopped-flow cell compartment. Reactant concentrations in the two loading syringes were 2-fold greater than the final concentrations in the observation chamber. (These final concentrations are reported in the figure legends). The reaction buffers for the experiments were 50 mM HEPES, pH 7.5, containing 10% glycerol.

Pre-steady-state Kinetic (Stopped-flow) Data Analysis

Rate constants in the rapid scanning stopped-flow kinetic experiments were determined by Robust Global Fitting of the spectra using software provided by OLIS, Inc. (28–31). For each concentration of ligand utilized, the data from at least five runs were averaged. In general, the substrate concentration dependences of the observed rate constants were fit to Equation 1 describing a one-step reaction (32) using the nonlinear regression analysis program SigmaPlot.

$$k_{obs}=k_1[S]+k_{-1} \quad \text{(Eq. 1)}$$

Rapid Chemical Quenched-flow Experiments

Rapid chemical quenched flow experiments were performed using a SFM-400/Q mode quenched-flow apparatus (BioLogic Science Instruments), equipped with a circulating water bath to control the temperature of the reactants. Samples were aged following an interrupted flow and collected using a "partial liquid collection method" as programmed according to the manufacturer's manual. Reactions were initiated by mixing 70 μl of the enzyme (in 10 mM HEPES, 10% glycerol, pH 7.5) with 70 μl of the substrate(s). After transiently stored in the intermixer volume, 40 μl of enzyme and the substrate(s) were used to purge the intermixer volume, and then enzyme (30 μl) and substrate(s) (30 μl) were flowed through the intermixer volume. (In all cases, the concentrations of enzymes and substrates cited in the text are those after mixing and during the enzymatic reaction.) Reactions were quenched with 60 μl of 0.28 M perchloric acid at various aging times. Quenched samples were immediately transferred into ice, vortexed, and centrifuged at 12,000 × *g* for 10 min and 4 °C. Protein pellets were discarded, and the supernatants were collected and stored at −70 °C until the next day's analysis. ALA concentration in the quenched samples (*i.e.* in 100 of 120 μl) was determined after the method of Lien and Beattie (33) with a few modifications. Specifically, the ether extraction step was eliminated, and an extinction coefficient of 34.9 ± 0.4 mM^{-1} cm^{-1}, estimated under the present assay conditions, was used to determine ALA concentration from the difference in absorbance at 552 and 650 nm.

For the determination of CoA concentration in the quenched samples, we developed a new, rapid, spectrophotometric assay, involving the use of pyridine nucleotide-based enzymatic cycling to improve sensitivity. The general principle of the assay is the coupling of the pyruvate dehydrogenase- and citrate synthase-catalyzed reactions (Fig. 1*A*). Upon the oxidation of pyruvate, the generated NADH in the pyruvate dehydrogenase-catalyzed reaction is "amplified" through CoA enzymatic recycling. Simply, the citrate synthase-catalyzed condensation of acetyl-CoA with oxalacetate recycles the CoA used in the pyruvate dehydrogenase-catalyzed reaction, thus achieving a far higher analytical sensitivity to determine CoA concentration. To perform the assay, a 600-μl reaction mixture, containing 20 mM HEPES, 3 mM $MgCl_2$,1 mM NAD^+, 0.2 mM thiamin pyrophosphate, 0.4 mM mercaptoethanol, 1 mM sodium oxalacetate, 10 mM sodium pyruvate, 0.15 unit/ml citrate synthase, 0.10 unit/ml pyruvate dehydrogenase, was prepared and incubated for 5 min at 30

°C. To this reaction mixture, in a 1-ml, 30 °C-thermostatted cuvette, a quenched sample (30 μl), previously neutralized with 8.4 μl of 0.5 M NaOH, was added, and the change in absorbance was monitored at 340 nm. Under these conditions and over the range of 0.1–2.0 μM CoA, the rate of NADH production is linearly dependent on CoA concentration (Fig. 1*B*).

Pre-steady-state Kinetic (Quenched-flow) Data Analysis

The amounts of CoA and ALA produced at different reaction (or aging) times were plotted against time and fitted, using the nonlinear least-squares regression analysis program Sigmaplot, to Equation 2 (32),

$$P_t = A(1 - e^{-k_b t}) + k_{ss} E_0 t \quad \text{(Eq. 2)}$$

where P_t represents the product concentration at an aging time t, A is the amplitude of the burst phase, k_b is the burst rate constant, k_{ss} is the steady-state rate constant, and E_0 is total enzyme concentration.

RESULTS

Rapid Scanning Stopped-flow Kinetic Analyses of the Reactions of ALAS with Glycine and ALAS with Glycine and Acetoacetyl-CoA

Under pseudo-first-order reaction conditions, with the glycine concentration in excess of ALAS, the reaction of glycine with ALAS is accompanied by the formation of a species absorbing at 415 nm. Global analysis of all the absorbance changes data collected from 312 to 543 nm yielded the absorption spectra for the initial, intermediate, and final species and revealed that the reaction of glycine with ALAS follows a three-step process (Fig. 2). There are no major absorption spectral changes other than those at ~415 nm. In fact, besides the increase in absorbance at 415 nm, the spectrum of the final species indicates just a slight red shift (to 422 nm) of this spectral band in relation to that of the initial species (Fig. 2*A*). We assigned the three phases of the reaction of ALAS with glycine to 1) formation of the enzyme-substrate (Michaelis) complex, 2) formation of the external aldimine, and 3) abstraction of the glycine *pro*-R proton associated with the production of a carbanion/quinonoid intermediate (EQ1). Binding of glycine to ALAS yielded the Michaelis complex, in which the PLP cofactor still formed the internal aldimine. The spectrum of the species assigned as the Michaelis complex exhibited solely a small red shift of the absorbance band associated with the ALAS Schiff base linkage. The formation of the assigned external aldimine was accompanied by an increase in absorbance at 422 nm, as previously reported for the ALAS-glycine external aldimine (20), whereas the phase proposed to be associated with the proton removal from glycine virtually exhibited no shift in the 422-nm absorbance. The rates for the first two phases appear to be dependent on glycine concentration, with a clear sigmoidal dependence for phase 2, which suggests cooperativity between the two ALAS active sites (Fig. 2, *B* and *C*). In contrast to the rates for phases 1 and 2, the third phase rate is independent of glycine concentration (even as high as 150 mM) with a value of 0.0019 s^{-1} (Fig. 2, *B–D*). This value is in excellent agreement with the rate of 0.0022 s^{-1} determined for the ALAS-catalyzed removal of tritium from [2-$^3H_2$]glycine (19).

Previously, we reported that in the presence of succinyl-CoA there is an over 90-fold rate increase in the reaction of ALAS with glycine. We proposed that succinyl-CoA promotes this rise in the rate constant by inducing a conformational change of ALAS toward a “closed conformation,” wherein the condensation between glycine and succinyl-CoA occurs (20). In an effort to understand the role of succinyl-CoA in promoting the reaction of glycine with ALAS, we analyzed this reaction in the presence of acetoacetyl-CoA. We reasoned that acetoacetyl-CoA, with the same C-chain length as succinyl-CoA and with an oxo function at

the C-3 position, would sustain, albeit to a lower extent, a change in ALAS conformation. The results in Fig. 3 indicate this to be the case. Since, at glycine concentrations lower than 80 mM, the small amplitude associated with the different phase rates resulted in low signal to noise ratios, all of the reactions were for glycine concentrations equal or higher than 80 mM (Fig. 3). The global analysis of the data for the reaction of 60 μM ALAS with 250 mM glycine plus 30 μM acetoacetyl-CoA at pH 7.5 and 30 °C reveals that the rates for the first and second steps of the three-step kinetic process are of the same order of magnitude as those for the reaction of ALAS with only glycine (Fig. 3*B versus* Fig. 2, *B* and *C*), suggesting that acetoacetyl-CoA does not have a significant effect on the formation of either the enzyme-glycine (Michaelis) complex or the external aldimine. In contrast, the rate of the third phase, which we assigned to correspond to the proton extraction from glycine, was raised at least 10-fold (Fig. 3*C versus* Fig. 2*C*). Taken together, these results suggest that acetoacetyl-CoA binding can induce a conformational change in ALAS, leading to the appropriate positioning of the catalytic base for the glycine proton abstraction.

Rapid Scanning Stopped-flow Kinetic Analysis of the Reaction of ALAS with ALA

When ALAS (60 μM) was reacted with ALA (2.0 mM) for 15 s at pH 7.5 and 30 °C, there was an increase in the absorbance of the 515-nm species. ALA concentration was required to be greater than 0.4 mM in order to have enough enzyme to yield measurable changes in absorbance and yet maintain pseudo-first order conditions. Global fitting of the data for the 15-s reaction revealed four kinetically discernible species (Fig. 4*A*). The rate constant for the first of the three-phase kinetic process did not exceed 7 s^{-1} (Fig. 4*B*), and we proposed that this step is the transformation of the Michaelis complex (ALA-ALAS) into the enzyme-ALA external aldimine, possessing the 422-nm absorbance maximum as the major spectral feature. Indeed, the spectrum of the first kinetic species (Fig. 4*A*) is distinct from that of the ALAS holoenzyme (which was actually identified as the first kinetically competent species in the reaction of ALAS with glycine and identical to that of the proposed ALAS-glycine Michaelis complex (Fig. 2*A*)). Thus, it appears that in the reaction of ALAS with ALA, the initial species corresponds to the ALAS-ALA complex, and its formation is terminated within the dead time of the stopped-flow instrument. The absorbance features of species 3 reveal those of a quinonoid intermediate, and the kinetics associated with its synthesis exhibit saturation with ALA with a maximum rate constant equal to 1.77 ± 0.01 s^{-1} (Fig. 4*C*). The fourth kinetically competent species appears to be a quinonoid intermediate, and the rate constant governing this third kinetic step is virtually independent of ALA concentration, with an approximate value of 0.17 s^{-1} (Fig. 4*D*).

Whereas the reaction of ALAS with ALA is dominated by the quinonoid intermediate (EQ_2) formation, the reaction of the enzyme with glycine is more recalcitrant to the delivery of the initial quinonoid intermediate (EQ_1). Only the presence of the succinyl-CoA substrate brings the rate of EQ_1 production to levels amenable for overall ALA biosynthesis. The differences between the glycine and ALA structures lie in the acyl chain length and a carbonyl group in ALA. To test whether the increased lability of the ALA C-5 position could be due to the electron-withdrawing effect of the adjacent carbonyl group, the reaction of ALAS with 5-aminopentanoate, in which the 4-carbonyl group of ALA has been replaced with a methylene group, was examined using rapid scanning stopped-flow spectroscopy at pH 7.5 and 30 °C (Fig. 5). Global fitting data analysis for the first 10 s of the reaction from 312 to 543 nm demonstrated two kinetically competent species with absorbance maxima at 420 nm (Fig. 5*A*), which were interconverted through a monophasic, exponential process. The observed rates were linearly dependent on 5-aminopentanoate concentration, and the data were fit to Equation 1, yielding values of 0.041 ± 0.001 m_M^{-1} s^{-1} and 0.25 ± 0.03 s^{-1} for k_1 and k_{-1}, respectively (Fig. 5*B*). The k_{-1} value determined from the global data fitting is, however, ~0.021 s^{-1} (Fig. 5*C*). The higher value for k_{-1} (0.25 s^{-1}) as the intercept on the *y*

axis (Fig. 5*B*), as dictated in Equation 1, is probably associated with the larger error from inferring k_{-1}. Thus, the dissociation constant, K_d, is about 0.51 mM and is lower than that of glycine for ALAS, previously reported to be 22 mM (23). In contrast to this 43-fold decrease, the dissociation constant of 5-aminopentanoate from ALAS is 20-fold greater than that of ALA (23), suggesting that the carbon chain length and a carboxyl group are key elements to induce the ALAS conformational change.

Kinetics of the ALAS Reaction: The Rate-limiting Step Occurs after CoA Production

To explore the events occurring at the active site and dissect the rate-limiting step, we performed chemical quenched-flow experiments to look for a pre-steady-state burst of product formation. Initially, we monitored CoA formation, since CoA is the first product to be released in the proposed ALAS reaction pathway (Scheme 1). To this end, we developed a new rapid and sensitive assay for CoA detection, which was based on coupling the reactions catalyzed by pyruvate dehydrogenase and citrate synthase (Fig. 1*A*). Increased sensitivity in the assay was attained through pyridine-nucleotide amplification, which, in turn, was directly coupled with CoA-utilizing reactions (Fig. 1*A*). Control experiments indicated that detection of CoA is linear in the range of product formed under our pre-steady-state conditions (Fig. 1*B*).

The time course for the forward reaction (at pH 7.5 and 20 °C) was determined by adding succinyl-CoA to ALAS preincubated with glycine to initiate the reaction. The final concentrations after mixing were 30 μM ALAS, 200 mM glycine, and 150 μM succinyl-CoA; given the K_m values of ALAS for glycine and succinyl-CoA of 23 mM and 2.3 μM, respectively, the reaction concentrations were selected to ensure saturation in relation to both substrates and multiturnover conditions. At various times after mixing, the reaction was quenched with perchloric acid (34) using a quenched-flow apparatus, and the CoA concentration was determined as described under "Experimental Procedures." The time course for production of CoA was biphasic (Fig. 6). A pre-steady state of CoA formation was observed with an amplitude of 0.16/enzyme site and a burst phase rate of 188 s^{-1}, which was followed by a much slower (about 5000-fold) rate of 0.034 s^{-1}, corresponding to steady-state turnover. These data indicate that a step occurring after catalytic condensation of glycine and succinyl-CoA and after CoA production was at least partially rate-limiting.

Pre-steady-state Kinetic Analysis of ALA Formation

Chemical quenched-flow studies were performed to investigate the kinetics of formation of ALA, which is the terminal product released in the ALAS-catalyzed reaction (Scheme 1). Pre-steady-state kinetic analyses were conducted at saturating concentrations of glycine and succinyl-CoA such that a burst in ALA product formation would indicate that a step after catalysis would be at least partially rate-limiting. Reactions (at 20 °C) were initiated either by adding succinyl-CoA (150 μM) to ALAS (30 μM) preincubated with glycine (200 mM) or adding succinyl-CoA (300 μM) to ALAS (60 μM) preincubated with glycine (200 mM) and were stopped at different times with perchloric acid (Fig. 7). The time courses associated with ALA formation were biphasic (Fig. 7) and were described by a burst phase with a rate of 18.7 ± 3.9 s^{-1} and a steady-state phase rate of 0.033 ± 0.007 s^{-1} (in the case of the reaction with 30 μM ALAS) and a burst phase with a rate of 26.7 ± 4.5 s^{-1} and a steady-state phase rate of 0.039 ± 0.005 s^{-1} (in the case of the reaction with 60 μM ALAS). The burst amplitudes for the two time courses were 0.12/enzyme. The value for the steady-state rate (0.035 ± 0.007 or 0.039 ± 0.005 s^{-1}) agrees with that calculated from the time course for CoA production (see above), and the k_{cat} (0.016 s^{-1}) was determined under steady-state conditions (35). The 500-fold or greater difference between the rate of chemical transformation (~18 s^{-1}) and the steady-state rate suggests that a step after the chemical transformation limits the ALAS reaction.

Kinetics of ALAS Reaction

As noted in the Introduction, rapid scanning stopped-flow analyses, under multiturnover conditions, indicated that reaction of ALAS with glycine and succinyl-CoA results in a pre-steady-state burst quinonoid intermediate formation (20). Since the analysis of multiturnover kinetics can be complex, we sought to examine more closely the events occurring at the ALAS active site by performing rapid scanning stopped-flow experiments with enzyme in excess over the substrate (*i.e.* under single-turnover conditions). Rapid scanning stopped-flow spectral data corresponding to the reaction of 60 μM ALAS preincubated with 5 mM glycine (*i.e.* ALAS-glycine complex) with 10 μM succinyl-CoA at pH 7.5 and 20 °C were collected at a rate of 1000 scans/s and were averaged to yield 62 scans/s. The reaction was analyzed by global fitting to all data from 312 to 543 nm for the first 1 s. The best fit is to a two-exponential process with rates of k_1 = 150 ± 30 s^{-1} and k_2= 2.54 ± 0.02 s^{-1} for the two phases. The absorbance spectrum for the initial species discloses a spectral band centered at 515 nm, typical of a quinonoid intermediate (Fig. 8*A*), thus indicating that the formation of the first quinonoid intermediate, EQ_1 (Scheme 1), is complete within the dead time (~2 ms) of the stopped-flow spectrophotometer and that the first kinetic step is associated with the decay of the EQ_1 intermediate. The absorbance spectra for the intermediate and final species reflect those of an external aldimine and a quinonoid species (EQ_2) (Fig. 8*A*). The loss of an absorbance at 515 nm in the intermediate species followed by its appearance in the final species led us to propose that the second kinetic step corresponds to the formation of the EQ_2 intermediate (Scheme 1). When the analysis was extended to the first 30 s of the reaction, the reaction was best described by a three-exponential process with k_1 = 2.5 ± 0.3 s^{-1}, k_2 = 0.47 ± 0.08 s^{-1}, and k_3 = 0.022 ± 0.005 s^{-1} for the three phases (Fig. 8*B*). The absorbance spectra for species 1 and 2 exhibit maxima at 420 and 515 nm, respectively, whereas the formation of species 3 and 4 is accompanied with disappearance of the 515-nm spectral band (Fig. 8*B*), indicating that the first kinetic step describes the formation of EQ_2. Further, the rate associated with this kinetic step (k_1 = 2.5 ± 0.3 s^{-1}) is in perfect agreement with the rate determined above for the second kinetic step occurring in the 1-s reaction (k_2 = 2.54 ± 0.02 s^{-1}), which was independently assigned with the production of EQ_2 (Fig. 8, *A versus B*). The disappearance of the 515-nm absorbance maximum of species observed with the transformation of species 2 into species 3, suggests that this step represents the conversion of EQ_2 into the ALA-PLP aldimine. The third kinetic step, governed by the k_3 = 0.022 ± 0.005 s^{-1}, appears to be associated with ALA release. In fact, this rate is in accord with the steady-state turnover number (0.016 s^{-1}) previously determined under the same reaction conditions (35).

Because most of the steady-state and transient kinetic studies from our laboratory have been performed at 30 °C, the ALAS reaction was also investigated in a single turnover at this temperature by reacting ALAS (60 μM) preincubated with glycine (10 mM) with succinyl-CoA (10 μM). The best global fitting of all data from 312 to 543 nm (Fig. 8*C*) is to a three-exponential process, and the rate constants for the three phases are k_1 = 5.37 ± 0.21 s^{-1}, k_2 = 1.54 ± 0.25 s^{-1}, and k_3 = 0.12 ± 0.01 s^{-1}. Remarkably, the k_{cat} (0.108 s^{-1})[3] is similar to the rate of the third kinetic step (k_3 = 0.12 ± 0.01 s^{-1}), reinforcing the idea that this kinetic step corresponds to product dissociation from ALAS.

DISCUSSION

Previous steady-state kinetic studies have indicated that the ALAS reaction pathway is ordered, with glycine binding first followed by succinyl-CoA and with the release of ALA after CoA and CO_2 (36). Pre-steady-state kinetic studies demonstrated that the rate-limiting

[3]J. Zhang and G. C. ferreira, unpublished data.

step in the ALAS-catalyzed reaction occurs following the binding of substrates and quinonoid species formation and possibly corresponds to the release of ALA or a protein conformational change associated with its release (20). The present transient kinetic analysis, involving a combination of rapid chemical quenched-flow and scanning stopped-flow methods, has provided a quantitative description of the overall ALAS reaction pathway. Global analysis of pre-steady-state data, collected under single turnover conditions, permitted us to distinguish the two postulated quinonoid intermediates (Scheme I). Further, a 500-fold difference between the rate of the chemical transformation and the steady-state rate validated our previous proposal that a step after ALA synthesis limits the rate of ALAS. Scheme II summarizes the results of the kinetic analyses of the ALAS reaction performed in this study.

In the absence of the succinyl-CoA substrate, the glycine reaction with ALAS is a three-step kinetic process, which we assigned to be the formation of the Michaelis complex and external aldimine intermediates, followed by the removal of the *pro*-R proton of glycine. As noted under “Results,” the formation of the Michaelis complex was not accompanied by a shift of the absorbance band centered at 415 nm, most likely indicating that the PLP cofactor still forms an internal aldimine in the Michaelis complex. The association rate constant for ALAS and glycine to form the Michaelis complex was calculated to be on the order of 10^4 to 10^5 m^{-1} s^{-1}, a value much lower than the rates reported for the formation of enzyme-substrate complexes (*i.e.* 10^7 to 10^8 m^{-1} s^{-1}) but reminiscent of that found for aromatic L-amino acid decarboxylase (38). The pK_a of the ALAS internal aldimine is ~ 10.3,[4] and, as with L-amino acid decarboxylase, the possibility remains that the 2×10^4 m^{-1} s^{-1} association rate constant results from a small portion of reactive substrate. It is conceivable that under the assay conditions (*i.e.* pH 7.5), the glycine substrate would remain mainly protonated and that the $\propto -NH_3^+$-glycine would associate with the aldimine-protonated form of ALAS, thus contributing with a minor route for Michaelis complex formation. In this scenario, and using the mechanism of L-amino acid decarboxylase as a model, one would expect that the pK_a of the $\propto -NH_3^+$ of glycine (*i.e.* 9.8) should decrease in the initial Michaelis complex, facilitating the conversion into the mechanistically favorable, unprotonated glycine-ALAS complex and the transaldimination to the external aldimine intermediate.

Clearly, prior to the nucleophilic addition, the amino group proton of glycine has to be removed. Among potential candidates involved in the proton removal are 1) the unprotonated phenolate oxygen of the PLP cofactor and 2) the imidazole nitrogen of the His^{282} residue. The determination of the three-dimensional structures of AONS and of the product-AONS complex led Webster *et al.* (39) to propose that 1) “the negatively charged phenolate oxygen is free and may accept a proton from the amino group of the incoming substrate” and 2) His^{207} in AONS (*i.e.* His^{282} in ALAS) is hydrogen-bonded to O-3 of the PLP ring and involved in a hydrogen bond network that could facilitate catalysis by enhancing the effect of the active site aspartate on the pK_a of the pyridinium ring N-1. A similar situation is plausible with ALAS, particularly given that the protonated phenolate oxygen would enhance the electrophilicity of the cofactor pyridine ring and accelerate the reaction of the incoming glycine substrate. Judging from the AONS x-ray structure (11, 39) and the ALAS three-dimensional structure model (35), it is also conceivable that the subsequent removal of the proton from the phenolate oxygen would involve the His^{282} hydrogen bond network. However, different residues have been proposed as the active site bases in other PLP-dependent enzymes (*e.g.* Tyr^{123} in *Treponema denticola* cystalysin (40, 41)), and, obviously, other possibilities for ALAS cannot be excluded at this point.

[4]J. Zhang and G. C. Ferreira, unpublished results.

Following transaldimination, which appears to occur with a rate constant greater than 0.1 s^{-1} (Fig. 2*C*), the released Lys^{313}, through its deprotonated ε-amino group, abstracts the glycine *pro*-R proton, yielding a carbanion intermediate, with characteristic quinonoid features (19) (Scheme I). A global analysis of the kinetic data (multiturnover and single turnover) permitted us to dissect kinetically competent species that had previously gone unnoticed. Namely, we could dissect the formation of the two postulated quinonoid intermediates (Scheme I). In this study, we calculated a rate of 0.0020 s^{-1} for the formation of the first quinonoid intermediate (EQ_1) (Scheme II). Previously, we had shown that ALAS catalyzes the removal of tritium from [2-$^3H_2$]glycine with an approximate rate constant of 0.0021 s^{-1} (19), which corroborates our assignment for the EQ_1 formation. The decay of this intermediate is very rapid (>15,000 m_M^{-1} s^{-1}) in the presence of succinyl-CoA. In fact, we hypothesize that succinyl-CoA induces an enzyme conformational change to a catalytically active conformation, which would position the Lys^{313} in proximity to lead to a rapid C-α proton abstraction from glycine and EQ_1 formation. And indeed, we estimate that succinyl-CoA accelerates the rate of glycine proton extraction and formation of EQ_1 ~250,000-fold.

Interestingly, and as predicted, acetoacetyl-CoA, an alternate and nonphysiological ALAS substrate, did not affect significantly the rate constants associated with formation of the Michaelis complex and external aldimine but did increase the rate associated with the glycine proton removal by at least 10-fold. These results suggest that although acyl-CoA derivatives have the molecular requirements to promote the extraction of the glycine *pro*-R proton, only succinyl-CoA combines the determinants conducive to the progress of the reaction, which is consistent with the stringent specificity of ALAS toward the second substrate, succinyl-CoA. Several other PLP-dependent enzymes (*e.g.* aspartate aminotransferase (42, 43), tryptophan synthase (44), *O*-acetylserine sulfhydrylase-A (45, 46), AONS (11, 39, 47), and 2-amino-3-ketobutyrate CoA ligase (12)) are known to sustain conformation transitions upon either substrate binding or product release. Of particular relevance are the changes undergone by the enzymes of the α-oxoamine synthase family, in which movement of the protein small domain occurs after substrate binding (39); a role for CoA binding was advanced as the triggering mechanism (12).

The burst of a 510-nm absorbing species upon the reaction of both substrates with ALAS suggested that the rate-determining step of the ALAS-catalyzed reaction must occur after quinonoid intermediate formation (20). However, results from this previous study did not allow a distinction to be made between the two postulated quinonoid intermediates (Scheme I). The global analysis of scanning stopped-flow absorbance results for single-turnover ALAS reactions has not only allowed the discrimination between the two quinonoid intermediates but also implied that neither CoA dissociation nor formation of the second quinonoid intermediate (EQ_2) could be rate-limiting. Actually, rates for these two steps are 180 s^{-1} and 5.4 s^{-1}, respectively (Figs. 6 and 8*C* and Scheme II); these values are much greater than the estimated k_{cat} (0.108 s^{-1}). Significantly, the release of ALA from ALAS occurs at a rate of ~0.12 s^{-1}, suggesting that the rate-limiting step in the overall reaction is the release of the third and final product (*i.e.* ALA). It is equally conceivable that the binding of ALA to ALAS promotes a change from an open to a closed conformation.

Strikingly, whereas glycine requires the binding of succinyl-CoA to ALAS to accelerate the C-2 proton abstraction from glycine and formation of EQ_2, binding of ALA is sufficient to promote the quinonoid intermediate formation (Fig. 4). The rate of formation of EQ_2 from the ALA-PLP aldimine is ~ 1,000-fold greater than EQ_1 formation from the glycine-PLP aldimine, and the dissociation constants of ALA and glycine from ALAS are also 1,000-fold apart, with the lowest value for the dissociation constant of ALA. These observations led us to hypothesize that the carbon chain length and the carboxylate group of the ligand determine the rate of quinonoid intermediate formation. And indeed, the reaction of 5-

aminopentanoate with ALAS is described as a monophasic kinetic process, with a dissociation constant ~20-fold lower than that of ALA and 43-fold greater than that of glycine (Fig. 5). Taken together, it appears that a critical C-chain length (*i.e.* C-5) and carboxylate group promote the nucleophilic reaction of ALA binding to ALAS and the exclusion of the catalytic base, Lys^{313}. However, the presence of the carbonyl group in ALA is also necessary to reach the formation of the quinonoid intermediate. We suggest that the cooperation of these three molecular factors of the ligand (*i.e.* carbonyl and carboxylate groups and carbon chain length) is required to bring about the protein conformational change and formation of the quinonoid intermediate in the reaction of ALA with ALAS.

In conclusion, we postulate that ALAS exists in two conformational states, an open conformation in which the substrates bind and a closed conformation induced by the binding of the second substrate, succinyl-CoA. We have demonstrated that the reaction of glycine with ALAS involves a three-kinetic step (*i.e.* formation of the Michaelis complex and external aldimine and removal of the glycine C-α proton from the external aldimine) and that the presence of succinyl-CoA accelerates this third step and thus EQ_1 intermediate formation. Analyses based upon transient, single turnover kinetics coupled to quenched-flow kinetics permitted us to substantiate the presence of two quinonoid species as intermediates in the ALAS-catalyzed reaction and to establish that ALA release is the rate-limiting step in the ALAS catalytic pathway.

REFERENCES

1. Ferreira, GC. Iron Metabolism: Inorganic Biochemistry and Regulatory Mechanisms. Ferreira, CG.; Moura, JG.; Franco, R., editors. Germany: Wiley-VCH, Weinheim; 1999. p. 15-34.
2. Ahktar, M.; Jordan, PM. Comprehensive Organic Chemistry: The Synthesis and Reaction of Organic Compounds. 1st Ed.. Haslam, E., editor. Vol. Vol. 5. Oxford: Pergamon Press; 1979. p. 1121-1144.
3. Ferreira GC, Gong J. J. Bioenerg. Biomembr. 1995; 27:151–159.
4. Nakajima O, Takahashi S, Harigae H, Furuyama K, Hayashi N, Sassa S, Yamamoto M. EMBO J. 1999; 18:6282–6289. [PubMed: 10562540]
5. Cotter PD, Willard HF, Gorski JL, Bishop DF. Genomics. 1992; 13:211–213. [PubMed: 1577484]
6. Bishop DF, Henderson AS, Astrin KH. Genomics. 1990; 7:207–214. [PubMed: 2347585]
7. Bottomley, SS. Wintrobe's Clinical Hematology. Lee, GR., editor. Baltimore: William & Wilkins; 1999. p. 1022-1045.
8. Alexander FW, Sandmeier E, Mehta PK, Christen P. Eur. J. Biochem. 1994; 219:953–960. [PubMed: 8112347]
9. Grishin NV, Phillips MA, Goldsmith EJ. Protein Sci. 1995; 4:1291–1304. [PubMed: 7670372]
10. Schneider G, Kack H, Lindqvist Y. Structure Fold Des. 2000; 8:R1–R6. [PubMed: 10673430]
11. Alexeev D, Alexeeva M, Baxter RL, Campopiano DJ, Webster SP, Sawyer L. J. Mol. Biol. 1998; 284:401–419. [PubMed: 9813126]
12. Schmidt A, Sivaraman J, Li Y, Larocque R, Barbosa JA, Smith C, Matte A, Schrag JD, Cygler M. Biochemistry. 2001; 40:5151–5160. [PubMed: 11318637]
13. Gable K, Slife H, Bacikova D, Monaghan E, Dunn TM. J. Biol. Chem. 2000; 275:7597–7603. [PubMed: 10713067]
14. Ikushiro H, Hayashi H, Kagamiyama H. J. Biol. Chem. 2201; 276:18249–18256. [PubMed: 11279212]
15. Zaman Z, Jordan PM, Akhtar M. Biochem. J. 1973; 135:257–263. [PubMed: 4543543]
16. Abboud MM, Jordan PM, Akhtar M. J. Chem. Soc. Chem. Commun. 1974:643–644.
17. Laghai A, Jordan PM. Biochem. Soc. Trans. 1977; 5:299–301. [PubMed: 302227]
18. Nandi DL. J. Biol. Chem. 1978; 253:8872–8877. [PubMed: 309883]
19. Hunter GA, Ferreira GC. Biochemistry. 1999; 38:3711–3718. [PubMed: 10090759]

20. Hunter GA, Ferreira GC. J. Biol. Chem. 1999; 274:12222–12228. [PubMed: 10212188]
21. Tan D, Ferreira GC. Biochemistry. 1996; 35:8934–8941. [PubMed: 8688429]
22. Ferreira GC, Neame PJ, Dailey HA. Protein Sci. 1993; 2:1959–1965. [PubMed: 8268805]
23. Gong J, Hunter GA, Ferreira GC. Biochemistry. 1998; 37:3509–3517. [PubMed: 9521672]
24. Tan D, Harrison T, Hunter GA, Ferreira GC. Biochemistry. 1998; 37:1478–1484. [PubMed: 9484217]
25. Ferreira GC, Dailey HA. J. Biol. Chem. 1993; 268:585–590.
26. Laemmli UK. Nature. 1970; 227:680–685. [PubMed: 5432063]
27. Hunter GA, Ferreira GC. Anal. Biochem. 1995; 226:221–224. [PubMed: 7793621]
28. Zhou X, Jin X, Medhekar R, Chen X, Dieckmann T, Toney MD. Biochemistry. 2001; 40:1367–1377. [PubMed: 11170464]
29. Sun S, Bagdassarian CK, Toney MD. Biochemistry. 1998; 37:3876–3885. [PubMed: 9521708]
30. Matheson IBC. Comput. Chem. 1990; 14:49–57.
31. Beechem J. Methods Enzymol. 1992; 210:37–54. [PubMed: 1584042]
32. Johnson KA. Enzymes. 1992; 20:1–61.
33. Lien L-F, Beattie DS. Enzyme (Basel). 1982; 28:120–132.
34. Farazi TA, Manchester JK, Gordon JI. Biochemistry. 2000; 39:15807–15816. [PubMed: 11123906]
35. Cheltsov AV, Barber MJ, Ferreira GC. J. Biol. Chem. 2001; 276:19141–19149. [PubMed: 11279050]
36. Fanica-Gaignier M, Clement-Metral J. Eur. J. Biochem. 1973; 40:19–24. [PubMed: 4359141]
37. Fersht, A. Structure and Mechanism in Protein Science: A Guide to Enzyme Catalysis and Protein Folding. New York: Freeman; 1998. p. 152-153.
38. Hayashi H, Tsukiyama F, Ishii S, Mizuguchi H, Kagamiyama H. Biochemistry. 1999; 38:15615–15622. [PubMed: 10569946]
39. Webster SP, Alexeev D, Campopiano DJ, Watt RM, Alexeeva M, Sawyer L, Baxter RL. Biochemistry. 2000; 39:516–528. [PubMed: 10642176]
40. Krupka HI, Huber R, Holt SC, Clausen T. EMBO J. 2000; 19:3168–3178. [PubMed: 10880431]
41. Clausen T, Huber R, Laber B, Pohlenz HD, Messerschmidt A. J. Mol. Biol. 1996; 262:202–224. [PubMed: 8831789]
42. Rhee S, Silva MM, Hyde CC, Rogers PH, Metzler CM, Metzler DE, Arnone A. J. Biol. Chem. 1997; 272:17293–17302. [PubMed: 9211866]
43. Jager J, Moser M, Sauder U, Jansonius JN. J. Mol. Biol. 1994; 239:285–305. [PubMed: 8196059]
44. Miles, EW.; Banik, U.; Ahmed, SA.; Parris, KD.; Hyde, CC.; Davies, DR. Biochemistry of Vitamin B_6 and PQQ. Marino, G.; Sannia, G.; Bossa, F., editors. Basel: Birkhauser; 1994. p. 113-117.
45. McClure GD Jr. Cook PF. Biochemistry. 1994; 33:1674–1683. [PubMed: 8110769]
46. Burkhard P, Tai CH, Ristroph CM, Cook PF, Jansonius JN. J. Mol. Biol. 1999; 291:941–953. [PubMed: 10452898]
47. Ploux O, Breyne O, Carillon S, Marquet A. Eur. J. Biochem. 1999; 259:63–70. [PubMed: 9914476]

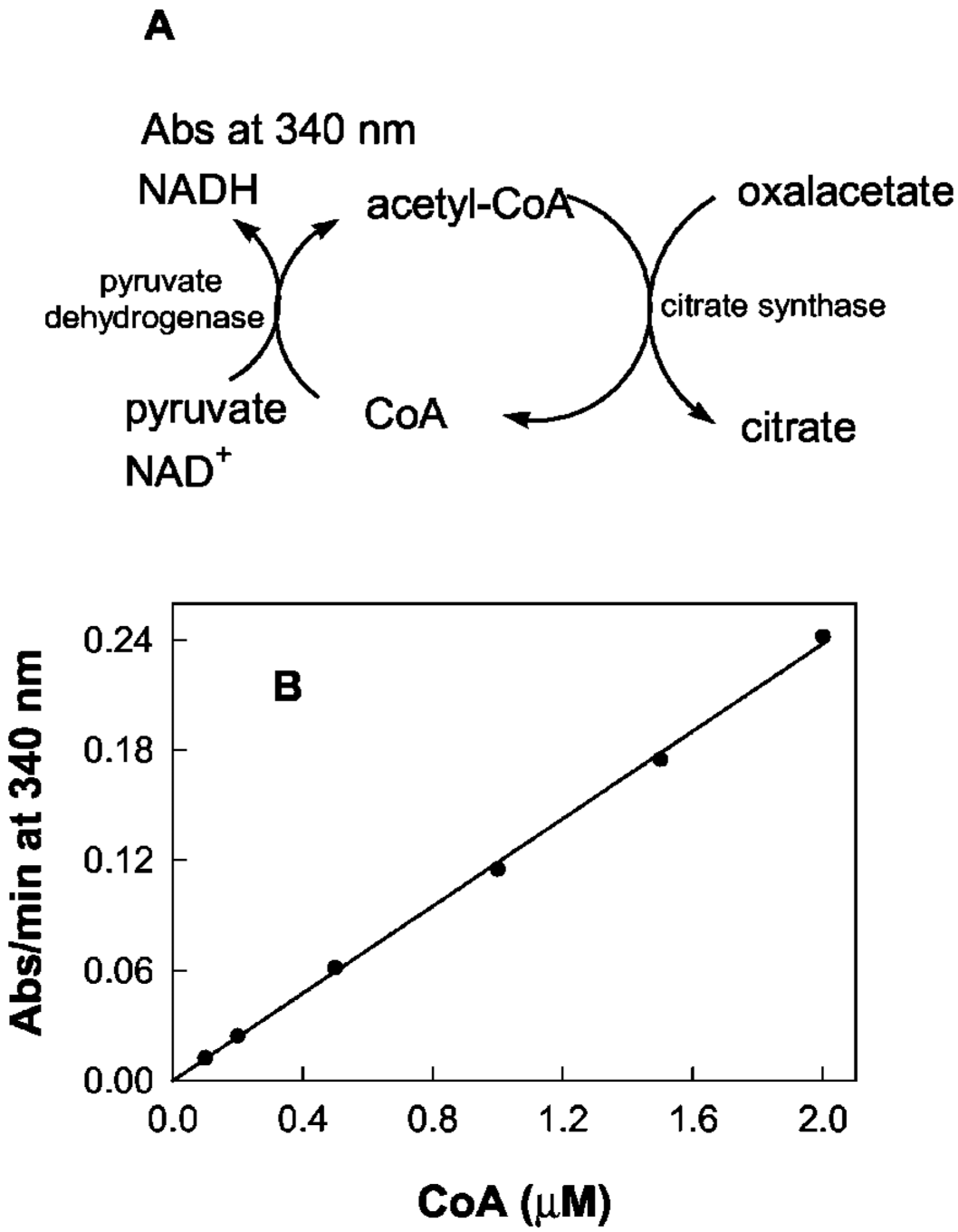

Fig. 1. Detection of CoA, the first product in the ALAS-catalyzed reaction, using NAD-NADH enzymatic cycling to increase assay sensitivity

A, scheme illustrating the coupling between CoA consumption and NADH production and amplification of NADH. The pyruvate dehydrogenase-citrate synthase-coupled reactions lead to CoA recycling and consequently to amplification of NADH (see "Experimental Procedures" for details). *B*, validation of the CoA detection assay. The rate of NADH formation is linearly proportional to CoA concentration with a slope of 0.119 ± 0.001 abs μ_M^{-1}. These data illustrate that for the range of CoA produced during the pre-steady-state analyses of the ALAS reaction, the pyridine nucleotide-enzymatic cycling assay yields NADH concentrations that are linearly dependent on the concentrations of substrates.

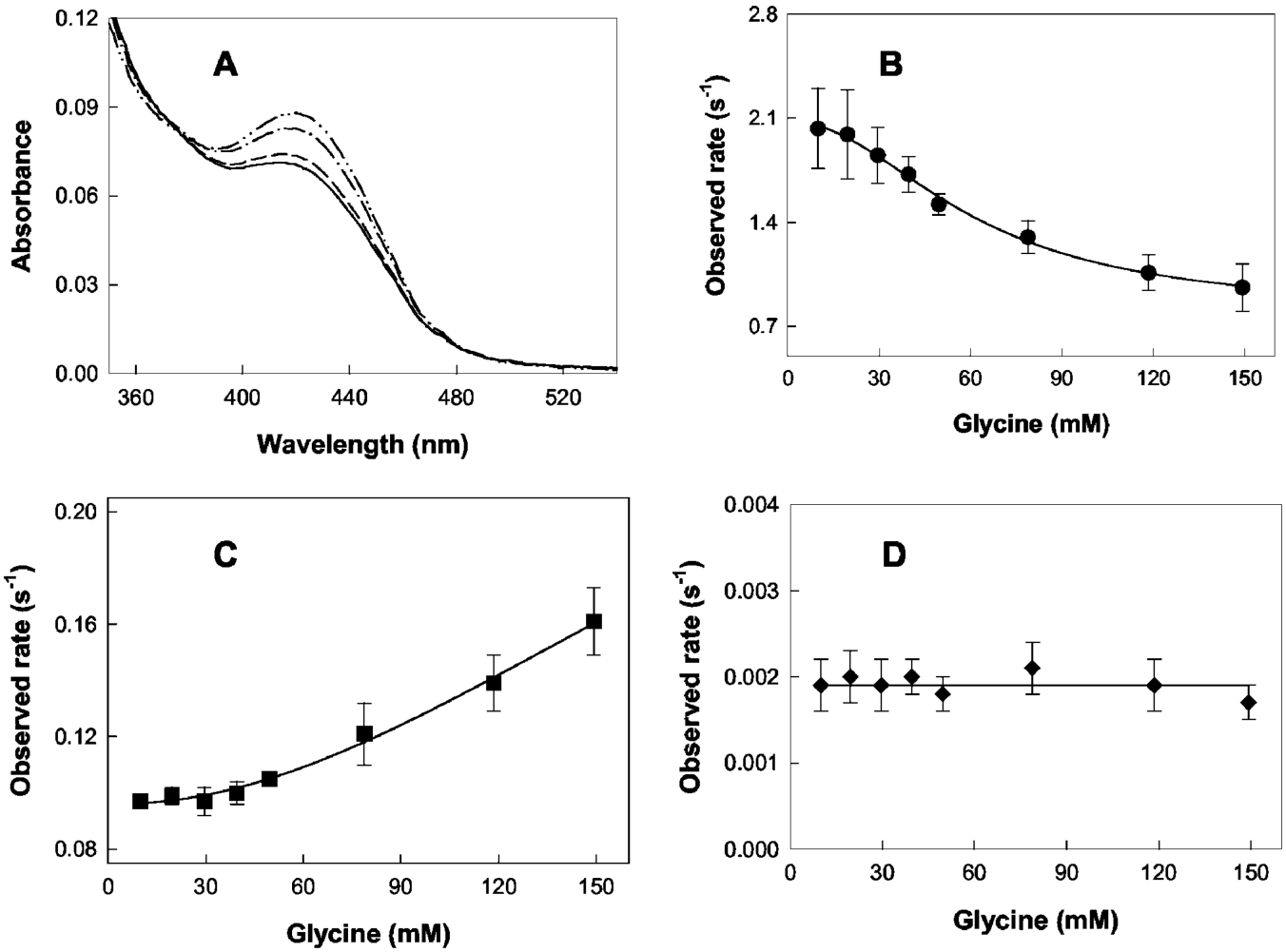

Fig. 2. Global transient state kinetic analysis of the reaction of ALAS with glycine

A, absorbance spectra for the four kinetically distinguishable species in the reaction of ALAS (50 μM) with glycine (50 mM) exhibiting pre-steady-state, triphasic kinetics: initial species (*solid*), intermediate (*dash*), final species (*dash-dot*), and species 4 (*dash-dot-dot*). The first kinetic phase is proposed to be the Michaelis complex formation, the second phase the external aldimine formation, and the third phase the proton removal from the glycine substrate. *B–D*, glycine concentration dependence of the first, second, and third phase rates, respectively. *Error bars* are plotted over the data points.

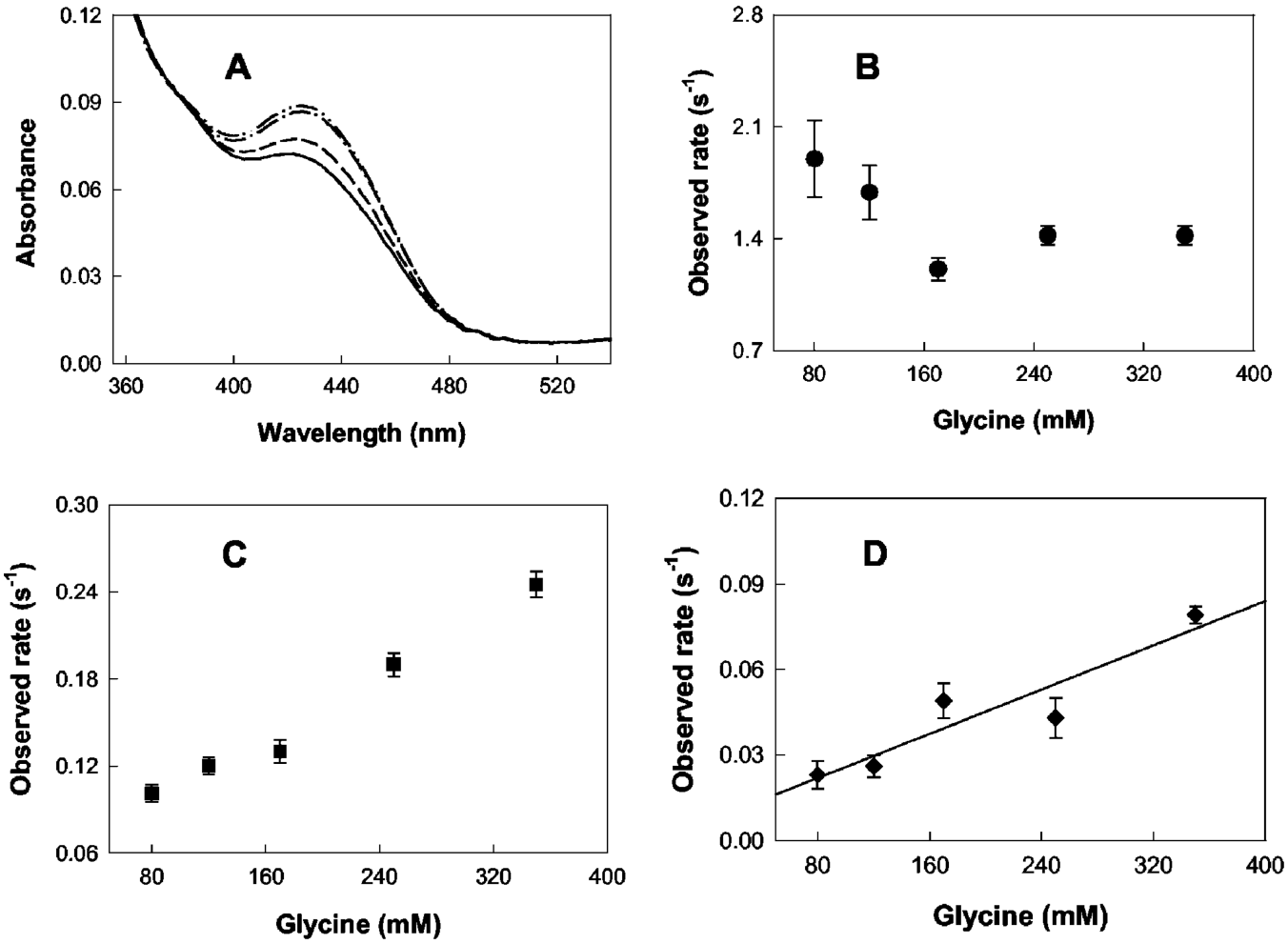

Fig. 3. Global transient state kinetic analysis of reaction of ALAS with glycine plus acetoacetyl-CoA

A, absorbance spectra for the four kinetically distinguishable species in the reaction of ALAS (60 μM) with glycine (250 mM) plus acetoacetyl-CoA (30 μM) displaying triphasic transient kinetics: species 1 (*solid*), species 2 (*dash*), species 3 (*dash-dot*), species 4 (*dash-dot-dot*); *B–D*, glycine concentration dependence of the first, second, and third phase rates, respectively. *Error bars* are plotted over the data points. Note the difference in the *y* axis scale in Fig. 3*D versus* Fig. 2*D*.

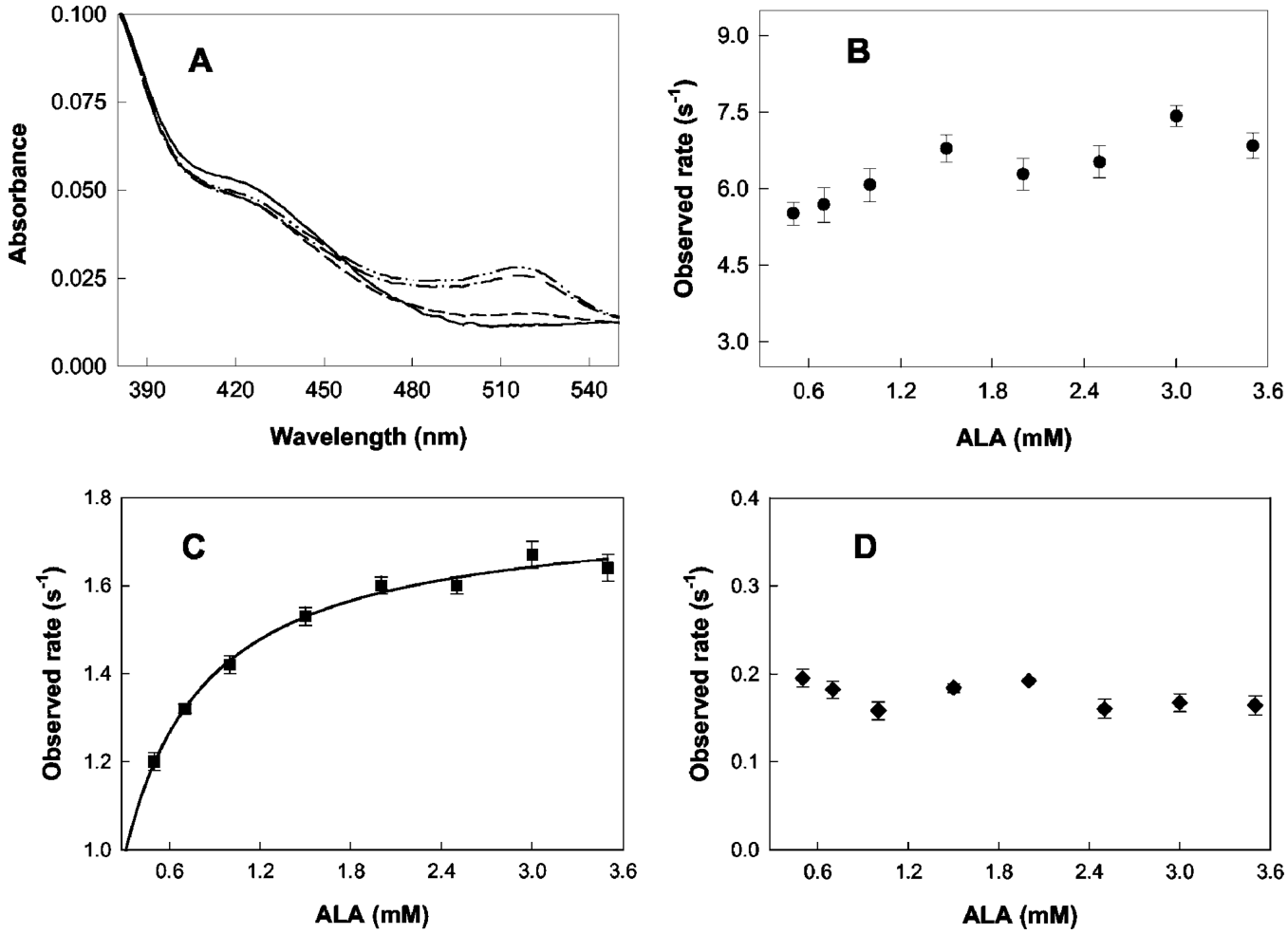

Fig. 4. Global transient state kinetic analysis of reaction of ALAS with ALA

A, absorbance spectra for four kinetically distinguishable species in the reaction of ALAS (50 μM) with ALA (2.0 mM): species 1 (*solid*), species 2 (*dash*), species 3 (*dash-dot*), and species 4 (*dash-dot-dot*). The reaction follows a three-exponential pre-steady-state kinetic process. The first kinetic phase is proposed to be the conversion of Michaelis complex into the ALA-PLP aldimine. The second phase is proposed to be associated with EQ_2 production from the external aldimine, and the third phase is proposed to correspond to a conformational change of the enzyme. *B–D*, glycine concentration dependence of the first, second, and third phase rates, respectively. *Error bars* are plotted over and partially obscured by the data points.

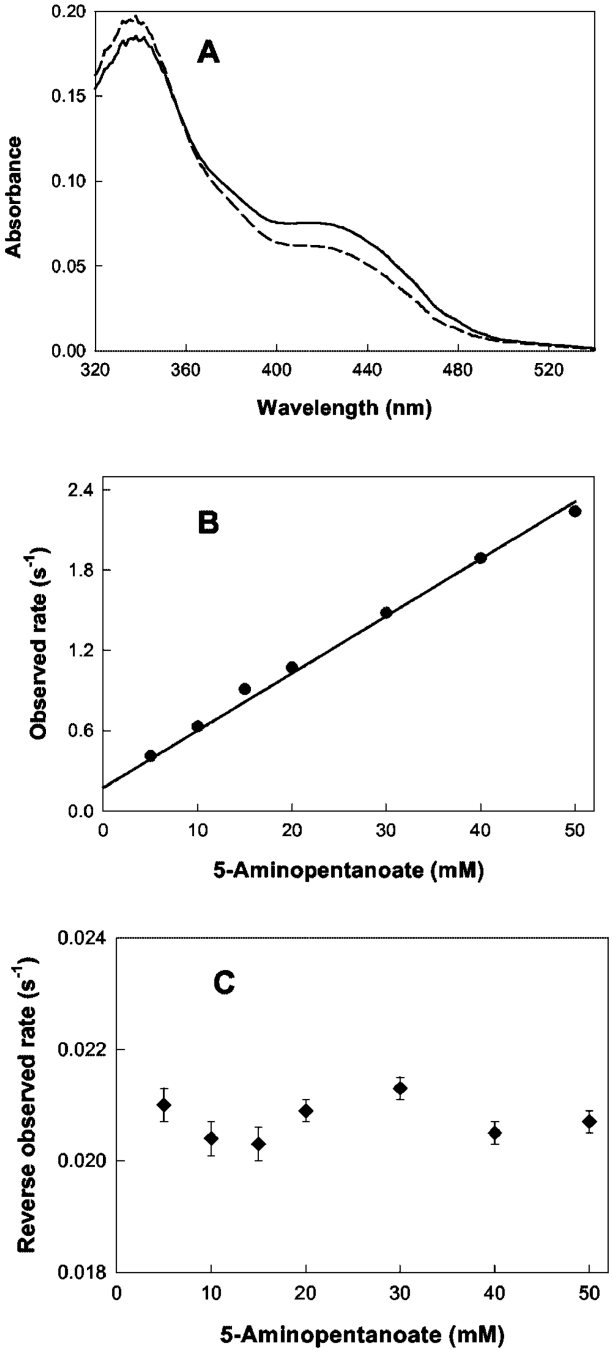

Fig. 5. Global pre-steady-state kinetic analysis of the reaction of ALAS with 5-aminopentenoate

A, absorbance spectra for the two species (initial species (*solid line*) and final species (*dashed line*)) in the pre-steady-state reaction of ALAS (60 μM) with 5-aminopentanoate (20 mM) as described by a monophasic kinetic process. *B* and *C*, 5-aminopentanoate concentration dependence of the forward and reverse rates, respectively.

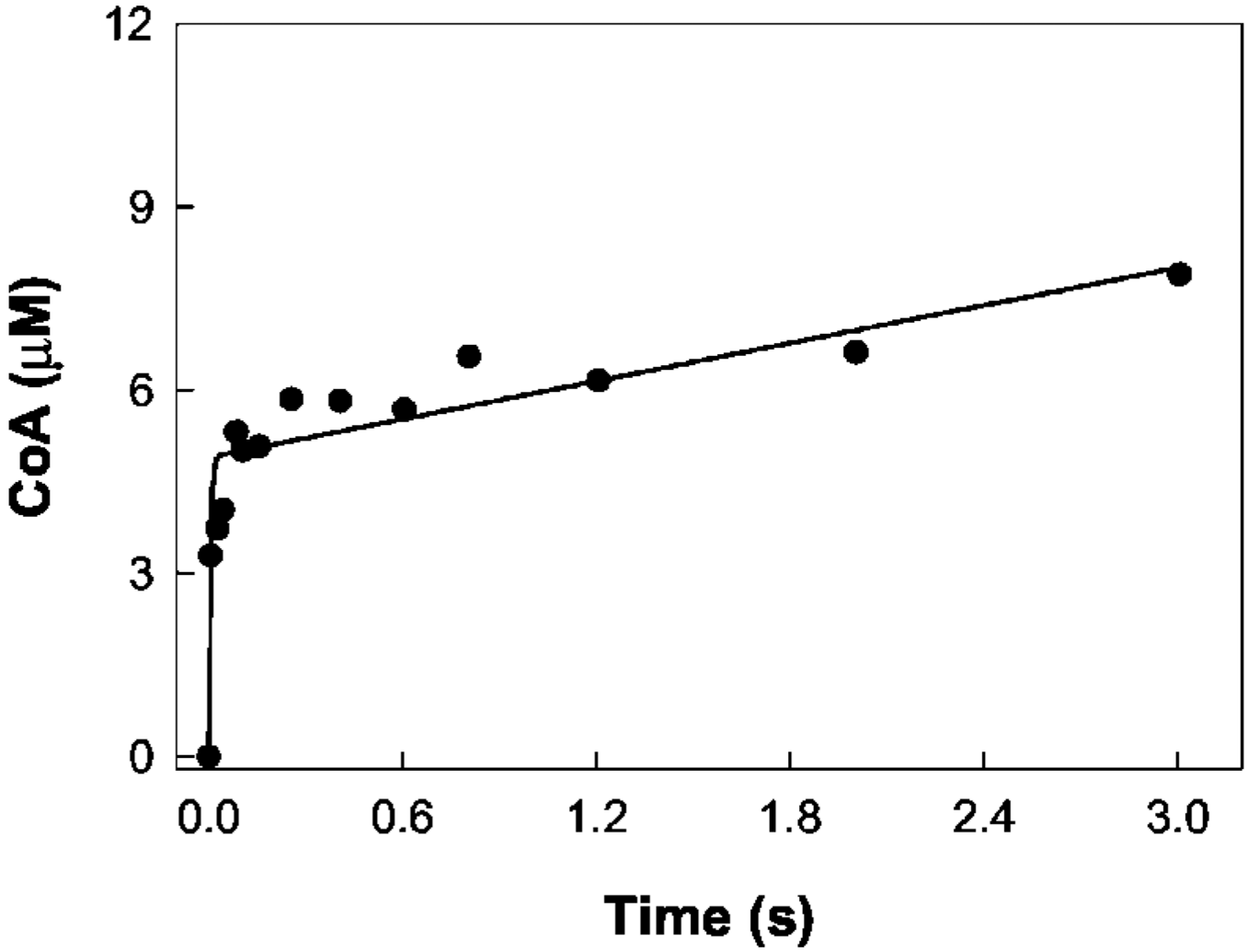

Fig. 6. Kinetics of pre-steady-state burst of CoA product in ALAS reaction

ALAS (30 μM) preincubated with glycine (200 mM) was quickly mixed with succinyl-CoA (150 μM) at 20 °C. The concentrations shown in *parentheses* are final concentrations after mixing. The reaction was quenched with perchloric acid (0.14 M) at various aging times, and the CoA concentration was determined as described under "Experimental Procedures." The *curve* represents the best fit to Equation 2 with a burst amplitude of 4.9 ± 0.2 μM, a burst rate of 188 ± 64 s^{-1}, and a steady-state rate of 0.034 ± 0.006 s^{-1}.

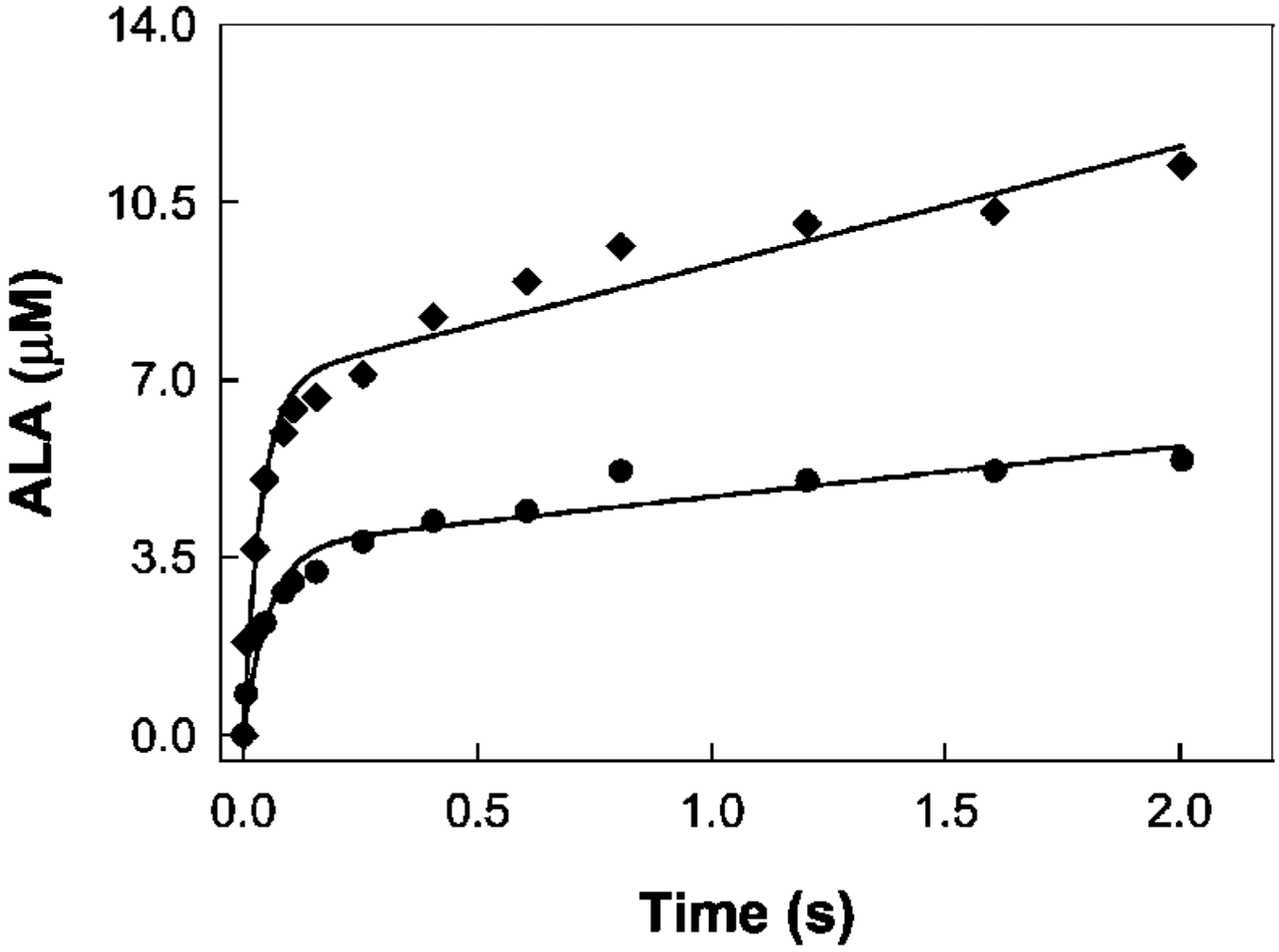

Fig. 7. Kinetics of pre-steady-state burst of ALA product in ALAS reaction

Typical time courses for ALA formation from the reaction at 20 °C of succinyl-CoA (150 μM) with ALAS (30 μM) preincubated with glycine (200 mM) (*circles*) and of succinyl-CoA (300 μM) with ALAS (60 μM) preincubated with glycine (200 mM) (*diamonds*). The reactions were quenched with perchloric acid (0.14 M) at various aging times, and the ALA concentration was determined as described under "Experimental Procedures." The concentrations shown in *parentheses* are final concentrations after mixing. Data for both time courses were fit using Equation 2. The rates and amplitudes for the fitted data are given under "Results."

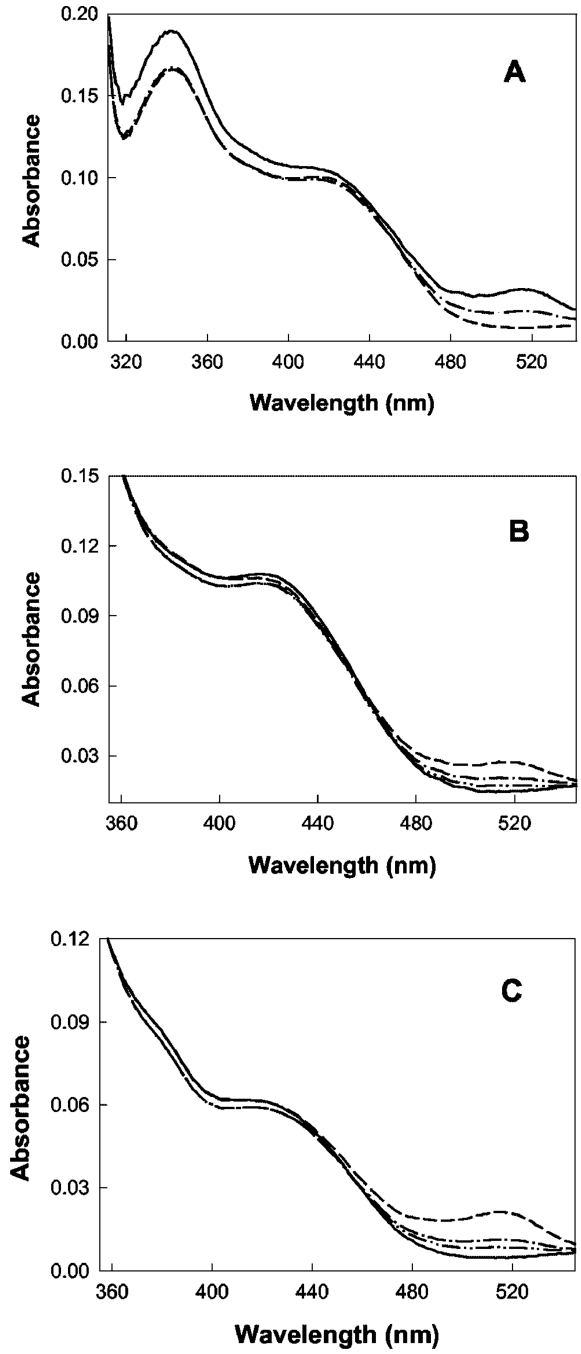

Fig. 8. Pre-steady-state single turnover in the ALAS reaction

A, absorbance spectra for three kinetically distinguishable species upon global fitting analysis of the data for the ALAS-glycine complex reacted with succinyl-CoA for 1 s at 20 °C: species 1 (*solid*), species 2 (*dash*), and species 3 (*dash-dot*). The first second of the reaction follows a biphasic exponential process, with the two phases ascribed to the decay of the PLP-glycine quinonoid (EQ_1) intermediate and the formation of PLP-ALA quinonoid (EQ_2) intermediate. *B*, absorbance spectra for four kinetically distinguishable species in the 30-s reaction of ALAS-glycine complex with succinyl-CoA at 20 °C: species 1 (*solid*), species 2 (*dash*), species 3 (*dash-dot*), and species 4 (*dash-dot-dot*). Whereas the first second of the reaction follows a biphasic exponential process, the 30-s reaction is best described by

a three-step exponential kinetic process. *C*, absorbance spectra for the four species in the pre-steady-state reaction of ALAS-glycine complex (60 μM) with succinyl-CoA (10 μM) at 30 °C exhibiting triphasic exponential kinetics: species 1 (*solid*), species 2 (*dash*), species 3 (*dash-dot*), and species 4 (*dash-dot-dot*). The global data fitting analysis was for the first 30 s of the reaction. The first kinetic phase is proposed to be the EQ_2 formation, the second phase the conversion of EQ_2 into the ALA-PLP external aldimine, and the third phase the dissociation of ALA from ALAS.

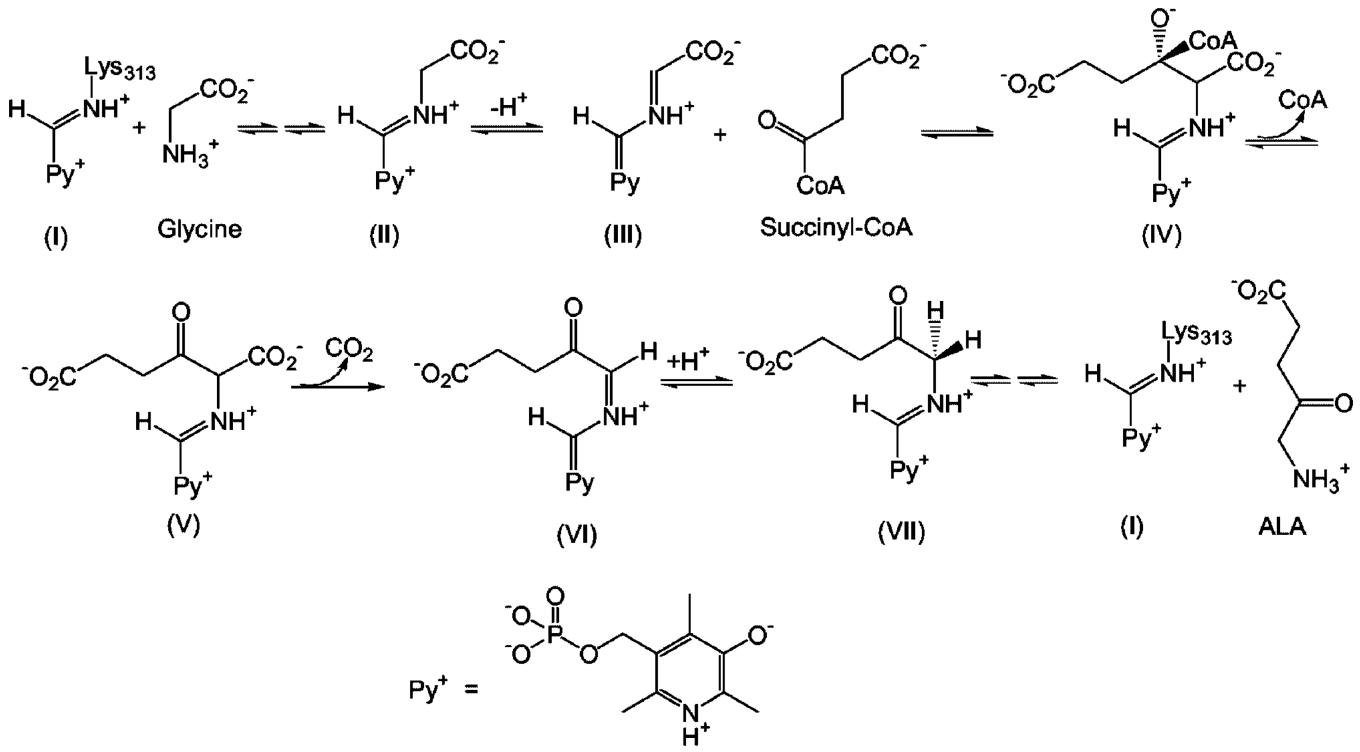

Scheme 1.

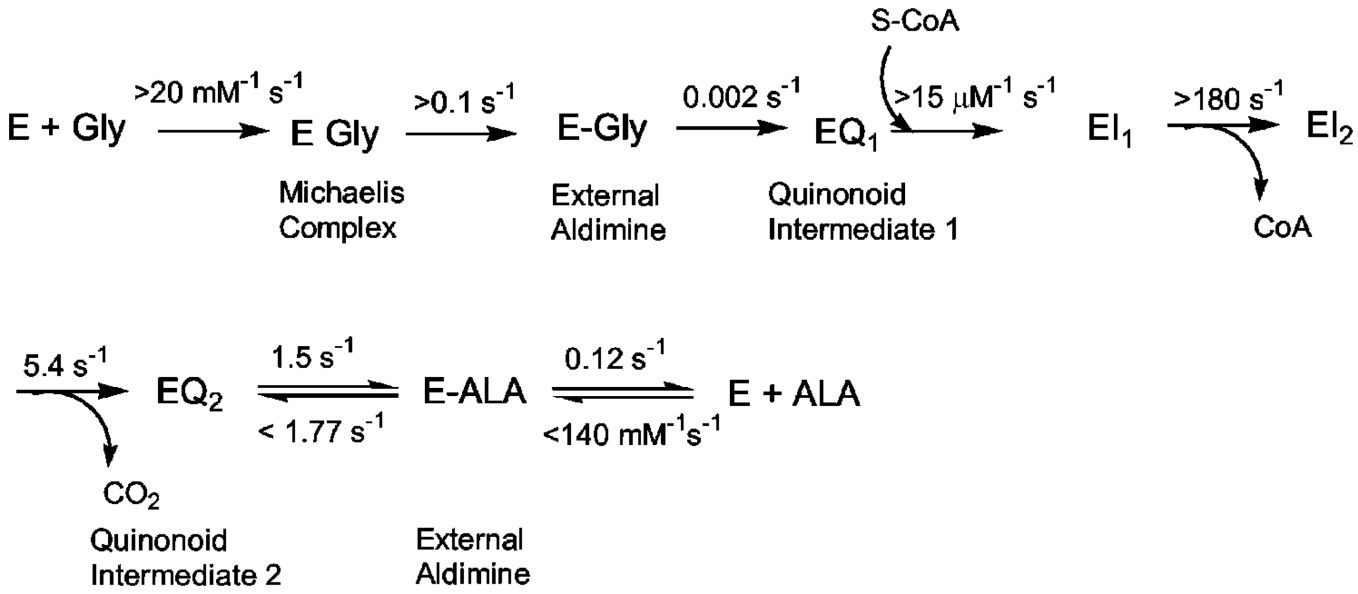

Scheme 2.